Journal of Engineering Research and Applied Science
Available at www.journaleras.com
Volume 9 (2), 2020, pp 1503-1520
ISSN 2147-3471 © 2020

Evaluation of Gördes zeolites in terms of mineralogical, geochemical and environmental effects

A. Vural[1,a], M. Albayrak[2]

[1] Gümüşhane University, Faculty of Engineering and Natural Science, Department of Geology, Gümüşhane, Turkey
[2]General Directorate of Mineral Researh and Exploration (MTA in Turkish), Çankaya, Ankara, Turkey

Accepted 1 October 2020

Abstract
In this study, zeolites in Gördes Basin were investigated in terms of their geological, mineralogical, geochemical and environmental effects. For his purpose, rock samples were collected from the area and investigated for geochemical and mineralogical properties of zeolite minerals using XRF (such as major element oxides, minor and trace elements) and XRD (for minerals). According to chemical analysis: the ranges of major oxides and loss of ignition (LOI) values are 0.1 to 1.6% for Na_2O, 0.2 to 12.4% for Mg, 1.5 to 15.5% for Al_2O_3, 32.2 to 73.7% for SiO2, 0.3 to 4.4% for K_2O and 0.9 to 17.0% for CaO and 6.55 to 30.30% for LOI. According to XRD analysis, zeolite minerals were mainly clinoptilolite and rarely is heulandite type. In some part of area, both of zeolite minerals, eg. clinoptilolite and heulandite were found together. SEM-EDX analysis is carried out on some samples, and both results obtained from XRD analysis are confirmed by SEM. On the basis of geological, geochemical, and mineralogical studies, general properties of the area were brought out. In addition, Gördes Basin has been environmentally evaluated in terms of zeolitisation and zeolite mineral types. It has been concluded that there is no negative environmental risk in this regard, since there are no minerals such as erionite with fibrous structure from zeolite group minerals. However, it is thought that the silica dust risk, which is frequently encountered in zeolitisation areas during mining operations in the field, should be taken into account. The risk of heavy metal contamination caused by zeolitisation, hydrothermal alteration was also examined in the area, and the presence of a radiogenic element/heavy metal pollution risk caused by zeolitisation, hydrothermal alteration and radiogenic element was determined especially for Cr, Rb, Sr, Pb, Th and U elements.

Keywords: Zeolites, Geochemistry, Mineralogy, Heavy Metal/Radiogenic Element Pollution, Gördes.

1. Introduction

Zeolite mineral was first introduced to the literature in 1750 by Swedish mineralogist Axel Fredrik Cronstedt. During his studies, the researcher observed that when the stilbite material was heated rapidly, a large amount of vapor was released from the water adsorbed by the material. Inspired by this observation, the researcher derived the word zeolite, which means "boiling rock" from Greek. Cause in Greek zeo means "boil" and lithos mean "rock / stone" [1]. Rocks rich in zeolite group minerals often explode and decompose when exposed to heat. Zeolites are secondary minerals formed only under conditions of high alkalinity (pH > 7), low temperature (<300°C) and low pressure due to diagenetic, deutric or hydrothermal processes affecting volcanic rocks. It can express the simple chemical composition in the form of Na, K and Ca hydrated bearing Al tecto-silicate. As can be understood, they are high in silica and alkali content, and clinoptolite, which is especially the K zeolite, represents the low temperature zeolite phase [2]. Mean that they are briefly basic, hydrous aluminosilicate group minerals. Zeolite minerals such as clinoptolite $[(Na_2,K_2,Ca)_3Al_6Si_{30}O_{72}.24H_2O]$, stilbite, analcime $[NaAlSi_2O_6.H_2O]$, natrolite, heulandite, chabazite $[CaAl_2Si_4O_{12}.6H_2O]$, erionite, offretite, mesolite, mordenite $[(Na_2,K_2,Ca)Al_2Si_{10}O_{24}.7H_2O]$, natrolite, paranatrolite, tetranatrolite, gonnardite, scolecite, mazzite, thomsonite are among the most well-known ones.. Zeolite minerals have a hollow and channeled lattice structure and they generally have an open aluminosilicate lattice with channels filled with water molecules and cations that are exchangable at temperatures below 100 ° C. Due to the loose lattice structure of zeolites, the cations in their bodies can easily be displaced, and they release the water in their channels and lattice spaces at high temperatures without deteriorating their lattice structures. These properties have made zeolites an important raw material with many uses, especially in the adsorption, ion exchange and dehydration industry [3]. The industrial and environmental use of zeolite is increasing so rapidly that the world natural zeolite production has almost exceeded 3 million tons annually in 2010s (Virta, R. L.

[a]Corresponding author; alaaddinvural@hotmail.com

2014. Zeolites. US Geological Survey Mineral Commodity Summary). China is the first in the world natural zeolite production, it is followed by Korea, Japan, Jordan and Turkey. There are approximately 42 known natural zeolite minerals with very different chemical compositions. These variations reflect various factors such as P-T conditions, chemistry of original material and pore water etc. [3, 4]. Natural zeolites are composed of various processes and lithology: a) saline-alkaline lacustrine deposits formed through essentially closed-system alteration of volcanic ash; b) vertical sedimentary sequences formed through open-system alteration and/or burial diagenesis of volcanic ash; c) hydrothermally altered volcanic or sedimentary rocks; and d) deep-sea sediments [5]. Considering that the primary rocks are volcanic, the close relationship between the formation environments and distribution of zeolites with volcanism is understood. Zeolites formed by hydrothermal, contact metamorphic, burial diagenesis and interaction of groundwater are generally more common in younger orogenic belts and in hot spots with volcanism accompanying thick sedimentation [4]. Most zeolite deposits are derived from tuffs and the first stage of zeolitization is considered to be the hydration of volcanic glass.

The study area containing zeolites is in Gördes and its vicinity (Manisa, Türkiye) in Western Anatolia. The zeolite formations in the field were developed in acidic tuffs. Two acidic tuff levels, each approximately 60 m thick, are located in the Miocene aged volcanic-sedimentary series of approximately 1000 m thickness [6–9]. Zeolite-bearing tuffs are white color and stratified and were formed in a lacustrine environment in Neogene, while fedding by volcanic activity in the form of ash flow [10].

There are some papers related to zeolite occurences in the region [6, 8, 9, 11, 12]. Some of them are mostly concerned with diagenetic, mineralogical, technological properties of zeolites. There are also studies using remote sensing techniques to search for zeolite and / or similar raw materials. Some of these studies were carried out especially for the investigation of zeolites in the Gördes basin [13–20]. The purpose of this study is to explain the geological, mineralogical and geochemical properties of the zeolites of Gördes and its vicinity (Gördes Basin) and also to evaluate the zeolites in the region from an environmental perspective.

2. Regional geology

Anatolia consists of many tectonic units, one of which is the Menderes Massif located in Western Anatolia. These tectonic units that make up Anatolia were formed by the deep burial of the northern edge of Taurids during the closure of the northern branch of the Neotethys [21, 22]. These basement rock of Tauride is stated to represent the northern continuation of the Neoproterozoic Pan-African basement of Afro-Arabian [23, 24], and affected by the "Kadomia" orogeny, and then an Andean type orogenic belt surrounding the northern Gondwana rim at the close of the Precambrian [25]. The Menderes Massif, is one of Turkey's most important massif and it was formed by interlocking Neoproterozoic-early Cenozoic sedimentary and magmatic rocks during Pan African and Alpine collisions[26–28]. The massif is divided into sub-massifs by Tertiary extensional grabens in an approximately E-W direction: The northern, central and southern sub-massifs. The study area is located in the Gördes-Demirci sub-massif in the north. The north of the Menderes massif is bordered by the İzmir-Ankara Zone consisting of marble and ophiolites and the south by the Lycian nappes[29]. In general, the massif is considered to consist of Neoproterozoic-early Cambria gneiss core, Palezoic schist cover and Mesozoic-lower Cenozoic carbonate dominant marbles from the bottom to the top [30, 31]. The core rocks are subjected to polymetamorphism and consist of partially migmatized metaclastic sequences (paragneiss and overlying micaschists, especially around Gördes) and late Proterozoic-early Camrian metagranitoid intrusions (orthogneisses, leucogranites, especially in the south of Gördes, Kula-Eşme regions) and eclogitized metagabbro stocks [27, 32, 33]. The core unit is unconformably covered by Paleozoic schists. The schist cover unit starts with the basal conglomerate consisting of meta conglomerate and meta quartzites, corresponding to the Supra-Pan African unconformity. The schist cover unit has undergone low grade metamorphism [30, 31, 34]. Palezoic cover schists have undergone metamorphism in their green facies. According to some researchers [23, 35], this metamorphism occurred in the Alp period and according to some [36] in the Early Triassic period.The Mesozoic-Lower Cenozoic marble cover unit, derived from the Anatolide-Tauride Neotethys platform, unconformably overlies the schist cover. This cover series consists of Lower Triassic chlorite schist, upper Triassic-Liassic interbedded marble and schist, Jurassic-lower Cretaceous massive dolomite, upper Cretaceous reddish pelagic limestones and Eocene wild flysch [31, 37, 38]. In the region, Phanereozoic cover sediments on the basis of the massif were not affected by any of these metamorphic processes [39].

It is thought that significant magmatic activity in the Menderes massif (nappes) occurred in the Proterozoic/Cambrian border [35], middle Triassic [40, 41] and Miocene [42, 43]. Also according to recent researhs on the Menderes massif the main metamorphic events that shaped the Precambrian basement of the massif are associated with the Kuunga orogeny and also Alpine metamorphism also led to limited retrograde events on basement units [28, 44].

Late Tertiary volcano-sedimentary basins are divided into three groups in Western Anatolia, where the Menderes massif is also located [45]. The Oligocene–Miocene molasse basins, the Neogene volcano-sedimentary basins and the Pliocene-Quaternary E–W-trending grabens. The Neogene volcano-sedimentary basins, one of them is subject to this study, have developed in NE-SW direction and are cut and displaced by active high angle normal faults with an approximately E-W direction, delimiting Plio-Quaternary grabens. Although there are many studies on Neogene Basins in the region, there is still not a complete consensus on the formation patterns of these basins.

2.1. Geology of study area

The study area is within the Gördes-Demirci Submassif (Fig. 1) of the Menderes Massif in the Gördes Basin, which trend at approximately right angles to the more topographically expressed, E–W-trending Alaşehir (Gediz) Graben and is located at an elevated plateau area bordered by rolling hills, c. 600 m above sea level. Neoproterozoic-early Cambrian orthogneisses and schists belonging to the core of the massif are located in the area. The core unit is covered by Paleozoic schist cover [28]. The northwestern margin of the basin includes extensive exposures of ophiolitic melange [46], an allochthonous unit that was initially emplaced southwards in latest Cretaceous–early Tertiary time from the northern Neotethys, rooted within the İzmir-Ankara suture zone (IASZ) [47]. The basement rocks are covered by late Cenozoic volcano-sedimentary units that were mainly deposited in lacustrine environments [45, 48–51]. The volcanic rocks and related Neogene sediments of the basin rest on continental blocks (mainly Menderes Massif metamorphics and suture zone rocks/IASZ). The Neogene volcanic activity in the basin is post-orogenic extensional [52]. The formation and lithological features of the basin have been interpreted differently by different researchers, and there are still unclear issues. This study is outside of the aforementioned discussions, and the definitions in [45] were used, taking into account the general acceptances. According to [45], in the basin, the Neogene starts with the Kızıldam Formation. This formation is conformably overlain by the Kuşlukköyü formation. Kuşlukköy formation interfingers with with Güneşli volcanics and they are cut by Kayacık volcanics in the center of the basin. All these units are unconformably covered by the Gökçeler formation. Late Miocene and actual sediments overlie the Gökçeler formation with unconformity. Kızıldam formation is the equivaleent of the formation defined as Kürköy by [53], and is an alluvial fan with reddish-brown conglomerates derived from the Metamorphic rocks of the Menderes Massif. In the western and northwestern part of the basin, the formation starts with mainly limestone dominant well-sorted conglomerates derived from the IASZ. Towards the center of the basin, the unit passes laterally towards the Kuşlukköyü formation. Based on the tourmaline minerals in the lechogranite pebbles in the Kızıldam formation, [42] has aged the unit to 24.2 ±0.8–21.1 ±1.1 Ma by K-Ar method. Therefore, the age of the unit has been suggested as early Miocene by the researchers.

The most common outcropping unit in the Gördes basin is the Kuşlukköy formation. The unit is of fluvio-lacustrine origin and consists of alternation of conglomerate-sandstone and sandstone-claystone. In the upper levels of the unit, north of Korubaşı village, there are marls and limestones. The Kuşlukköyü formation contains coal occurences in the western part of the basin, around the villages of Çıtak and Dağdere villages. For this reason, this region has been distinguished as a separate unit by some authors[48]. The formation is also intercalated with acid tuffs that is observed along a zone in the west of the basin from north to south. The early Miocene age has been given to the formation based on radiometric data [45]. Güneşli Volcanics crop out in a very large area in the basin, especially in the northern part of the basin. These volcanics, in which some of the zeolitisations in the region developed [7, 9, 18, 19], consist of pinkish white rhyolitic dykes and lava flows and rhyolitic proclastics towards the north of the Gördes basin (Gördes lake and its vicinity). The formation was called Kobaklar Volcanism by Göktaş, (1996). The pyroclastic rocks of the unit interfinger with the the Kuşlukköyü Formation. Tuff intercalations are 1-2 meters thick in the south of the basin and reach up to 30 meters towards the north of the basin. These acidic rocks are correlated with the dacitic to rhyolitic volcanic rocks of the Kayacık Volcanics in the center of the area (in the southwest of Gördes city). These rocks are also equvialent of Azimdağı Volcanics [48, 54]. The age of Güneşli volcanics was obtained as 19 Ma using biotite and feldspar Ar / Ar method by Purvis et al., (2005).

The Kayacık Volcanics crop out in southwest of Gördes City, the center of basin. Rocks are greenish yellow colored and are composed of mainly dacitic to rhyolitic

volcanic necks and associated lava flows and minor pyroclastic rocks interfingering with the Kuşlukköyü formation and in some locations the necks cut the Kuşlukköyü formation. Kayacık Volcanics were previously named as Azimdağı Volcanics [48, 54] and as central volcanics [56]. According to [57] (K-Ar method) and [55] (Ar/Ar method), these volcanics aged 18.4 ±0.6–16.3 ±0.5 Ma and 21.71±0.04–17.6±0.1 Ma respectively. The Gökçeler Formation crops out the wes¬t and souteast of Gördes City. The formation is consist of conglomerates, pebblestones, sandstones, siltstones and marls. It has a fluvio-lacustrine character and unconformably overlies the Kuşlukköyü Formation. The unit has been aged as middle Miocene, taking into account field observations, stratigraphic relationships and equivalents in the region [45]. The youngest units in the area are Late Miocene (?)-Plio-quaternary sediments.

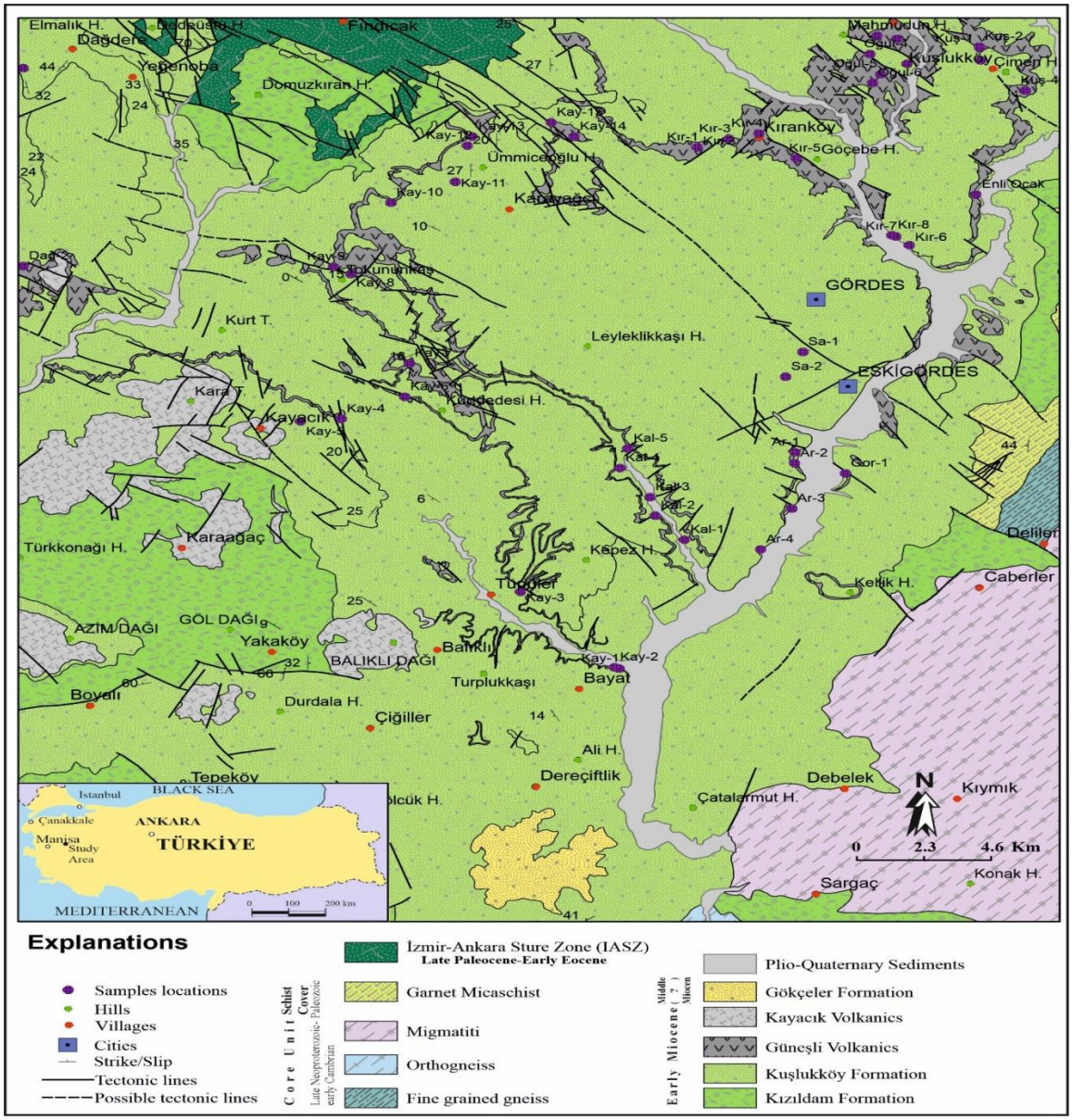

Figure 1. Geology of study area (modified after [45, 48]) and sample locations

2.2. Material and method

In this study, field studies for geological and geochemical purposes were carried out and the zeolite bearing samples were collected. Thin sections were prepared from the samples collected for mineralogical and petrographic examination of the rocks. In addition, samples were prepared for X-ray Diffraction (XRD), X-Ray Fluorescence (XRF) and Scanning Electron Microscopy coupled with Energy Dispersive X-ray (SEM-EDX) analysis. Most of the sample preparation processes were carried out

in the Mineral Analysis and Technology Laboratory of the General Directorate of Mineral Research and Exploration (MTA's Lab.). Samples are collected from all the potentially zeolite bearing units were prepared for XRD analysis by crushing and then grinding in an agate ball mill. During the sample preparation process for SEM-EDX analysis, the samples selected for analysis were covered with 350 A gold in order to obtain better quality images by increasing their conductivity. Subsequently, relevant analyzes were carried out. The determination of mineral types of zeolites was carried out by XRD and SEM-EDX analysis with the support of petrographic studies. Mineralogical-petrographic studies, XRD and geochemical analysis by X-Ray fluorescence spectrometry were mainly conducted in the laboratories of the MTA's Lab. SEM-EDX analyses were conducted in Laboratories of Turkish Cement Manufacturers' Association (LOTCMA).

Zeolite samples from the study area were analyzed by means of Powder X-ray diffraction (XRD) using a Rigaku-Geigerflex model diffractometer with monochromatic Cu Kα radiation operated at 40 kV and 30 mA, scanning from 2 to 70° 2 theta with a step size of 0.02° and a counting time of 1 s/step and mineralogical determinations were carried out using MDI/JADE6 software.

Types and characterizations of the zeolite minerals such as morphology, type, chemistry etc. were investigated using SEM-EDX in LOTCMA. During the analysis, it was taken SEM images and obtained EDX spectrum. X-ray fluorescence spectrometry (XRF) was used to determine the major and trace element concentration samples from the area. Element abundances were measured on fused discs and pressed powder pellets, respectively, using an automated Rigaku X-ray fluorescence spectrometer at LOTCMA. Loss on ignition (LOI) was determined by heating a separate aliquot of rock powder at 900 ^{o}C for 2 h. The geochemical properties of zeolites and geological settings of the related rocks were determined by using GCDKit 4.1 open source software by using the obtained geochemical data. IBM SPSS software v.19 was used for the statistical evaluation of the data.

3. Results and discussion

In the Gördes Basin, Neogene volcano-sedimentary sediments unconformably overlie Menderes massif metamorphics and IASZ units. The Neogene in the region begins with the Kızıldam formation during the Early Miocene period. On the Kızıldam formation, the Kuşlukköy formation comes with a lateral transition relationship in some regions. Güneşli volcanics, which spread over wide areas in the region, are laterally transitive with Kuşlukköy formation. Kayacık volcanics cut these units in different parts of the field. These volcanics are calcalkaline in character. Middle Miocene (?) Aged Gökçeler formation rests unconformably on these units. The youngest units of the basin are the late Miocene-Plio-Quaternary sediments (Fig 1). Although there is a very different opinion about the stratigraphy of sedimentary rocks in the field, [45]'s work, which has a simpler narrative, is taken into account in this study so that the confusion in the field does not distract the reader. However, the detail map of the field and formation relations can be found in [48]'s work. In the Gördes Basin, in the study on zeolites, of zeolite minerals, mostly clinoptilolite and less hoylandite and analcime bearing levels are observed in Güneşli Volcanics and Kayacık Volcanics (Fig. 2) [9, 58].

Figure 2. Zeolitization at lower part of Dedetepe hill. a) Upper level of Güneşli Volcanics' tuff which contains zeolite, b) same place from different view

3.1. Mineralogical evaluations

To investigate of geological, mineralogical and geochemical properties of zeolite from the region,

samples were collected and analyzed using XRD, SEM-EDX, and XRF. According to XRD measurements, mostly clinoptilolite and less heulandite, lesser extent analcime as zeolite minerals were determined. With these minerals, smectite group clay minerals, mica, quartz, feldspar and the amorphous material was also detected (Table 1 and 2).

Table 1. XRD Results of the sample

Samples	Minerals	Samples	Minerals
Gör.1	Clinoptilolite, amorphous materials	Kay.3	Heulandite, amorphous materials.
Oğul.1	Zeolite group mineral (heulandite-clinoptilolite), mica, quartz, smectite group clay minerals	Kay.4	Heulandite, amorphous materials.
Oğul.2	Zeolite group mineral (heulandite- clinoptilolite), amorphous materials	Kay.5	Clinoptilolite, amorphous materials.
Oğul.3	Heulandite, mica, smectite group clay, amorphous materials	Kay.6	Quartz, Zeolite group mineral (?Mordenite), mica.
Oğul.4	Clinoptilolite, mica, smectite group clay, amorphous materials	Kay.7	Clinoptilolite, amorphous materials.
Oğul.5	Clinoptilolite, mica, amorphous materials	Kay.8.	Clinoptilolite, Opal-CT, smectite group clay, mica, amorphous materials.
Oğul.6	Clinoptilolite, amorphous materials	Kay.9	Clinoptilolite, amorphous materials.
Enli Ocak	Zeolite group mineral (heulandite- clinoptilolite), amorphous materials	Kay.10	Quartz, amorphous materials.
SA.1	Feldspar, Zeolite group mineral (heulandite-clinoptilolite), mica	Kay.11	Quartz, amorphous materials.
SA.2	Zeolite group mineral (heulandite-clinoptilolite), mica, smectite group clay, amorphous materials	Kay.12.	Dolomite.
AR.1	Zeolite group mineral (heulandite-clinoptilolite), mica, smectite group clay, amorphous materials	Kay.13.	Clinoptilolite, smectite group clay, amorphous materials.
AR.2	Zeolite group mineral (heulandite-clinoptilolite), mica, amorphous materials	Kay.14.	Clinoptilolite, amorphous materials.
AR.3	Zeolite group mineral (heulandite- clinoptilolite)	Kay.15	Zeolite group mineral (heulandite-clinoptilolite), smectite group clay, amorphous materials.
AR.4	Zeolite group mineral (heulandite-clinoptilolite), amorphous materials	Kır.1.	Clinoptilolite, mica, quartz, amorphous materials.
KAL.1	Zeolite group mineral (heulandite-clinoptilolite), Opal-CT, smectite group clay, mica, amorphous materials	Kır.2	Clinoptilolite, amorphous materials.
KAL.2	Zeolite group mineral (heulandite-clinoptilolite), amorphous materials	Kır.3	Clinoptilolite, amorphous materials.
KAL?3	Zeolite group mineral (heulandite- clinoptilolite), amorphous materials.	Kır.4	Clinoptilolite, amorphous materials.
KAL.4	Zeolite group mineral (heulandite- clinoptilolite), mica, amorphous materials.	Kır.5	Clinoptilolite, amorphous materials.
KAL.5	Zeolite group mineral (heulandite- clinoptilolite), mica	Kır.6	Clinoptilolite, amorphous materials.
Kay.1	Heulandite, feldspar, mica, smectite group clay, amorphous materials.	Kır.7	Clinoptilolite, amorphous materials.
Kay.2	Heulandite, mica, smectite group clay, amorphous materials.	Kır.8	Zeolite group mineral (heulandite-clinoptilolite), quartz, feldspar, mica, amorphous materials.

SEM-EDX analysis were performed on 2 of the selected samples to determine the morphology, type, chemistry etc. of the zeolite minerals. Micromorphological images of clinoptilolite and smectite minerals as well as amorphous substance were obtained via SEM. SEM analysis on zeolites samples confirmed the XRD results and reveal that clinoptilolite minerals well-developed as plate in gaps and crack (Fig. 3). According to EDX analysis, peaks of K, Na, Ca, Al, O and Si were observed, that refers to the mineral clinoptilolite $[(Na_2,K_2,Ca)_3Al_6Si_{30}O_{72}.24H_2O]$ (Fig 3). In some back-scattered electron images of zeolite samples, platy clinoptilolite minerals, smectite minerals and the presence of globular amorphous material was also observed (Fig. 3).

When EDX analysis performed at different the points, in addition to K, Na, Ca, Al, O and Si peaks, increasing Mg peaks were observed that refers to smectite minerals.

When zeolite minerals are evaluated morphologically, zeolite minerals such as clinoptolite in plate-like structure/morphology were found in SEM analyzes, and no zeolite minerals in the form of fiborous crystals were found.

3.2. Geochemical evaluation

The samples analyzed for major (Na_2O, MgO, Al_2O_3, SiO_2, K_2O, CaO, TiO_2 and total FeO) and some trace element (V, Zn, Sr, Y, Zr, etc.) using XRF for 29 elements and, pH and lost of ignition (LOI) of these samples were also determined. The descriptive statistics (minimum, maximum, mean and standart deviation) of the 29 determined in samples are collectively listed in Table 3.

pH of the samples are in the range 6,97 to 9,91 which refers neutral to slightly basic. Loss of ignitions (LOI) values of the samples range between 6,55 and 30,30% with an average of 9,50. In the simplest definition,

zeolitisation can be defined as the process of change that volcanic materials undergo by absorbing water as a result of hydrothermal alteration. Therefore, it is an expected result that the LOI values of zeolites are high, and the results obtained have confirmed this. These values also show that rocks in the area were exposed to intensely hydrothermal alteration.

Table 1. Schematic representation of XRD data

Samples/ Minerals	**Clino**	**ZG(H-C)**	**ZG(?M)**	**Heu**	**Mica**	**SGC**	**Feld**	**Q**	**Dol**	**OPCT**	**AMORP**
Gör.1	■										■
Oğul.1		■			■	■		■			
Oğul.2		■									■
Oğul.3				■	■	■					■
Oğul.4	■				■	■					■
Oğul.5	■				■						■
Oğul.6	■										■
Enli Ocak		■									■
SA.1		■			■		■				
SA.2		■			■	■					■
AR.1		■			■	■					■
AR.2		■			■						■
AR.3		■									
AR.4		■									■
KAL.1		■			■	■				■	■
KAL.2		■									■
KAL?3		■									■
KAL.4		■			■						■
KAL.5		■			■						
Kay.1				■	■	■					■
Kay.2				■	■	■					■
Kay.3				■							■
Kay.4				■							■
Kay.5	■										■
Kay.6			■		■			■			
Kay.7	■										■
Kay.8.	■				■	■				■	■
Kay.9	■										■
Kay.10								■			■
Kay.11								■			■
Kay.12.									■		
Kay.13.	■					■					■
Kay.14.	■										■
Kay.15		■				■					■
Kır.1.	■				■			■			■
Kır.2	■										■
Kır.3	■										■
Kır.4	■										■
Kır.5	■										■
Kır.6	■										■
Kır.7	■										■
Kır.8		■			■		■	■			■

Clino: Clinoptilolite, ZG(H-C):Zeolite group mineral (heulandite-clinoptilolite, ZG(?M):Zeolite group mineral (?Mordenite), Heu:Heulandite, SGC: Smectite group clay, Feld:Feldspar, Q:Quartz, Dol:Dolomite, OPCT:Opal C-T, AMORP:Amorphous materials.

When the results of XRF analysis are evaluated, in the term of the major oxides, SiO_2 values range 68-73.9% omitting one basaltic rock, mean all rocks show acidic characters except one. For the other major oxides, it was determined that the MgO concentrations ranged between 0.2 and 12.40 and the average was 1.21 ppm, the Na_2O contcentrations ranged between 0.1 and 1.60 and the average was

between 0.43 ppm, the Al2O3 contcentrations were between 1.50 and 15.50 and the average was 11.68 ppm, the K_2O contcentrations were between 0.30 and 4.40 and the average was 2.58. ppm, CaO contcentrations were between 0.90 and 17.00 and an average of 3.40 ppm, TiO2 contcentrations ranged between 0.1 and 0.20 and an average of 0.1 ppm, and FeOt contcentrations were betweent 0.20 and 2.20 and the average was 1.03 ppm (Table 3). The distribution ranges of the major oxides and trace elements were analyzed by plotting boxplot diagrams (Fig 4). When Boxplot diagrams are examined, (when the sample is removed from the community, which alone affects the general trend of the sample communityit) is understood that both major oxides and trace elements show deviations from the normal distribution due to hydrothermal alteration, zeolitization. Na_2O, MgO, Al_2O_3, TiO2, FeOt, V, Cr, Zn, Rb and Pb have pozitif skewness (Fig. 4), others show either slightly negative skewness or a distribution close to normal distribution. It can be said that those which have positive skewness show enrichment with the mentioned parameters. In other words, these parameters were more affected by the alteration/zeolitization process than the others.

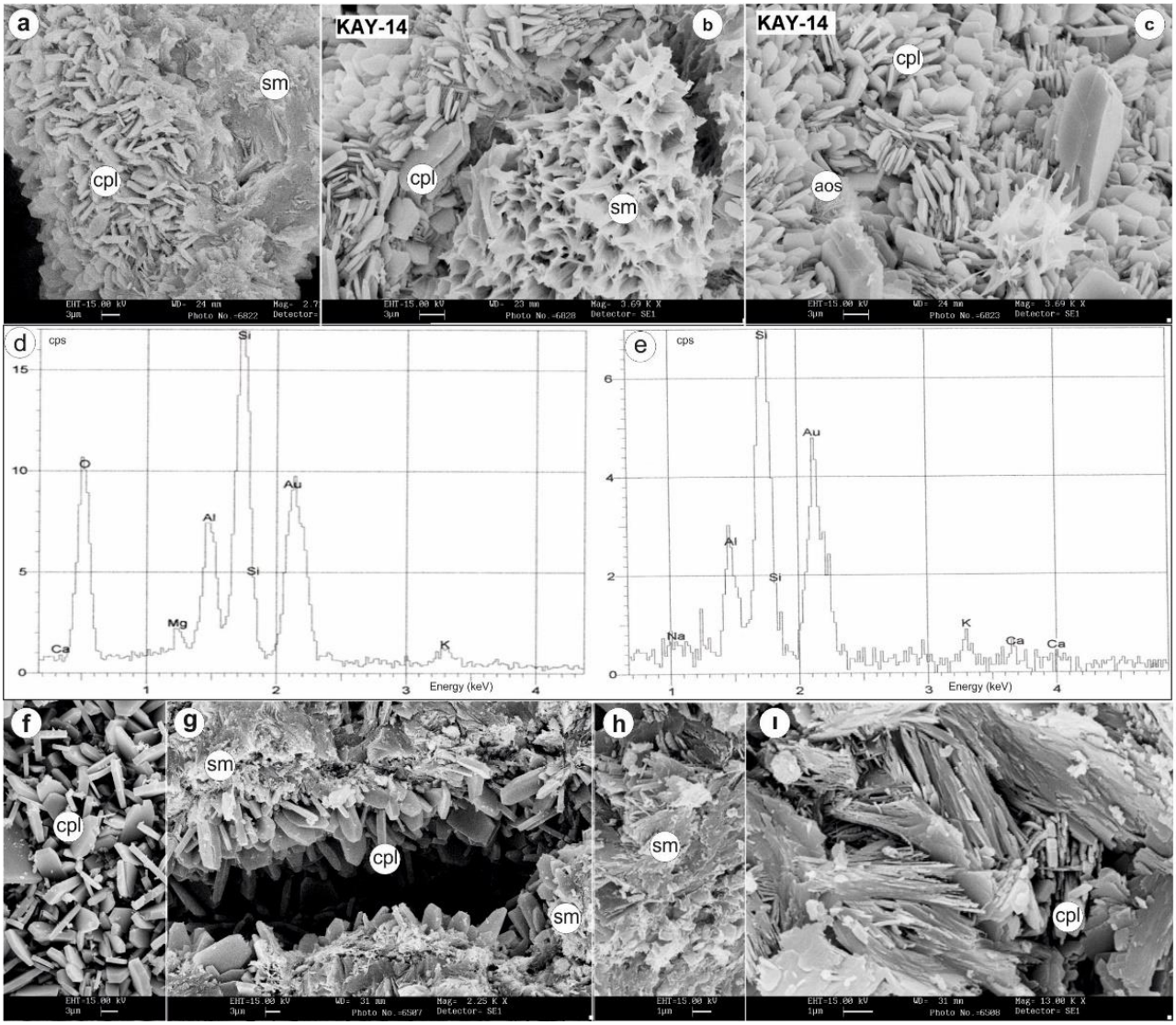

Figure 3. Back-scattered electron images showing aspects of zeolite group minerals, and its EDX graphs from some location a) clinoptilolite and smectite togetter, b) well-developed smectite and platy clinoptilolite minerals c) clinoptilolite platy minerals, smectite minerals and globular amorphous substance d) EDX graph showing smectite, e) EDX graph showing clinoptilolite, f) platy clinoptilolite different locality from the study area, g) well developed platy clinoptilolite minerals in gaps and cracks of tuff, h) entirely smectite containing samples ı) ongoing development of the clinoptilolite

Table 2. Descriptive statistics of major oxides and some trace elements (major oxides percent, trace elements in ppm)

	N	Minimum	Maximum	Mean	Std. Deviation	Variance	Skewness		Kurtosis	
	Statistic	Statistic	Statistic	Statistic	Statistic	Statistic	Statistic	Std. Error	Statistic	Std. Error
pH	29	6.97	9.91	8.67	0.66	0.44	-0.79	0.43	0.77	0.85
LOI	29	6.55	30.30	9.52	4.16	17.34	4.71	0.43	24.14	0.85
Na_2O	29	0.10	1.60	0.43	0.40	0.16	1.84	0.43	2.96	0.85
MgO	29	0.20	12.40	1.21	2.19	4.80	5.10	0.43	26.81	0.85
Al_2O_3	29	1.50	15.50	11.68	2.26	5.13	-3.23	0.43	15.22	0.85
SiO_2	29	32.20	74.10	69.59	7.52	56.59	-4.67	0.43	23.68	0.85
K_2O	29	0.30	4.40	2.58	1.02	1.04	-0.23	0.43	-0.30	0.85
CaO	29	0.90	17.00	3.40	2.73	7.45	4.69	0.43	24.02	0.85
TiO_2	29	0.10	0.20	0.10	0.02	0.00	5.39	0.43	29.00	0.85
FeOt	29	0.20	2.20	1.03	0.50	0.25	0.47	0.43	-0.12	0.85
V	18	12.00	34.00	17.61	6.03	36.37	1.31	0.54	1.72	1.04
Cr	5	91.00	6322.00	1413.60	2744.97	7534845.30	2.23	0.91	4.98	2.00
Zn	28	14.00	80.00	35.86	15.48	239.76	1.16	0.44	1.20	0.86
Rb	29	33.00	290.00	134.38	69.40	4815.96	0.89	0.43	0.33	0.85
Sr	29	39.00	2336.00	591.69	396.37	157105.44	3.11	0.43	13.58	0.85
Y	27	10.00	57.00	28.30	11.40	130.06	0.88	0.45	0.40	0.87
Zr	29	59.00	139.00	99.10	18.62	346.88	0.14	0.43	0.04	0.85
Nb	7	22.00	36.00	29.57	4.89	23.95	-0.62	0.79	-0.49	1.59
Ba	28	132.00	1289.00	565.86	335.22	112370.05	0.67	0.44	-0.61	0.86
Pb	25	24.00	147.00	57.44	31.38	984.84	1.33	0.46	1.56	0.90
Nd	11	20.00	37.00	28.55	6.23	38.87	-0.07	0.66	-1.70	1.28
Th	26	13.00	34.00	23.65	5.48	30.00	-0.25	0.46	-0.38	0.89
U	5	10.00	20.00	13.20	4.09	16.70	1.59	0.91	2.27	2.00

In order to examine the effects of hydrothermal alteration/zeolitization processes that the volcanic rocks in the field are exposed to, SiO_2 versus other major oxides diagrams (Harker variation diagrams) were created (Fig. 4). Major element distributions are illustrated on Harker variation diagrams where Al_2O_3, MgO, CaO and FeOt decrease with increasing SiO_2 and display negative trends (Fig. 5) compatible with the magmatic differentiation. Contrary to expectation related zeolitization, Na_2O decrease with increasing SiO_2 and display poor negative correlation with increasing SiO_2 but this negativity is not seen clearly. K_2O increase with increasing SiO_2 and display positive trends compatible with the alteration process and zeolitization.

On the Zr/TiO_2 versus SiO_2 diagram of Winchester and Floyd, (1977) the zeolite bearing volcanic rocks are mainly rhyolitic, rhyodacitic and less commonly trachytic composition (Fig. 5a) and they are in the subalkaline, calc-alkaline in character [45]. On the Nb/Y versus Zr/Ti diagram of Pearce, (1996) limited samples (due to Nb and Y absence) are commonly trachytic composition and less commonly rhyolitic, dacitic composition (Fig. 5b). These findings are consistent with previous studies in the field.

According to molar Na_2O-K_2O-Al_2O_3 triangular diagram, all samples display metaluminous/peraluminous and potassic trend compatible with alteration and zeolitization process (Fig. 5c).

Considering the spider patterns normalized lower continental crust [61], volcanic rocks are clearly enriched in LREE/incompatible elements and unfractionated HREE patterns, which are similar with the upper continental crust rather than the lower crust (Fig 5d).

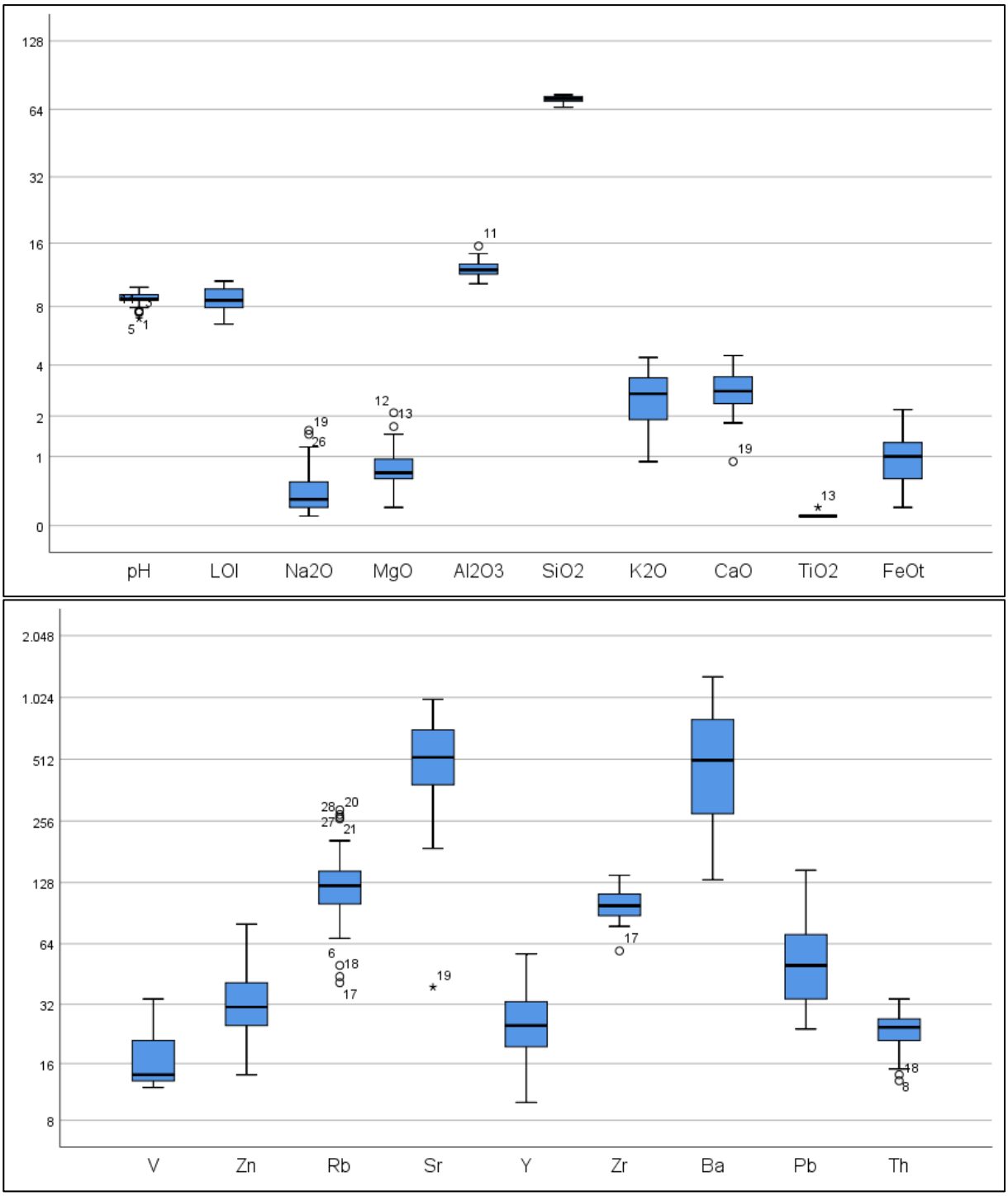

Figure 4. Boxplot diagrams of a) major oxides and b) trace elements

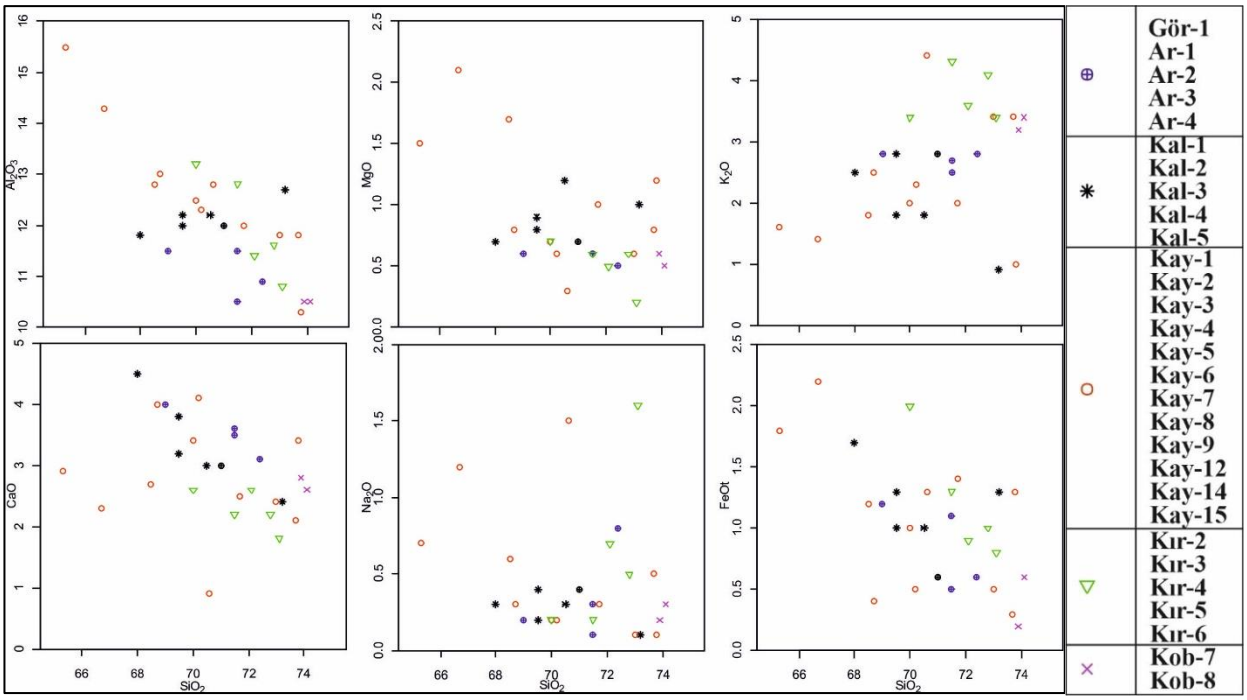

Figure 5. Diagrams of SiO_2 vs other major oxides

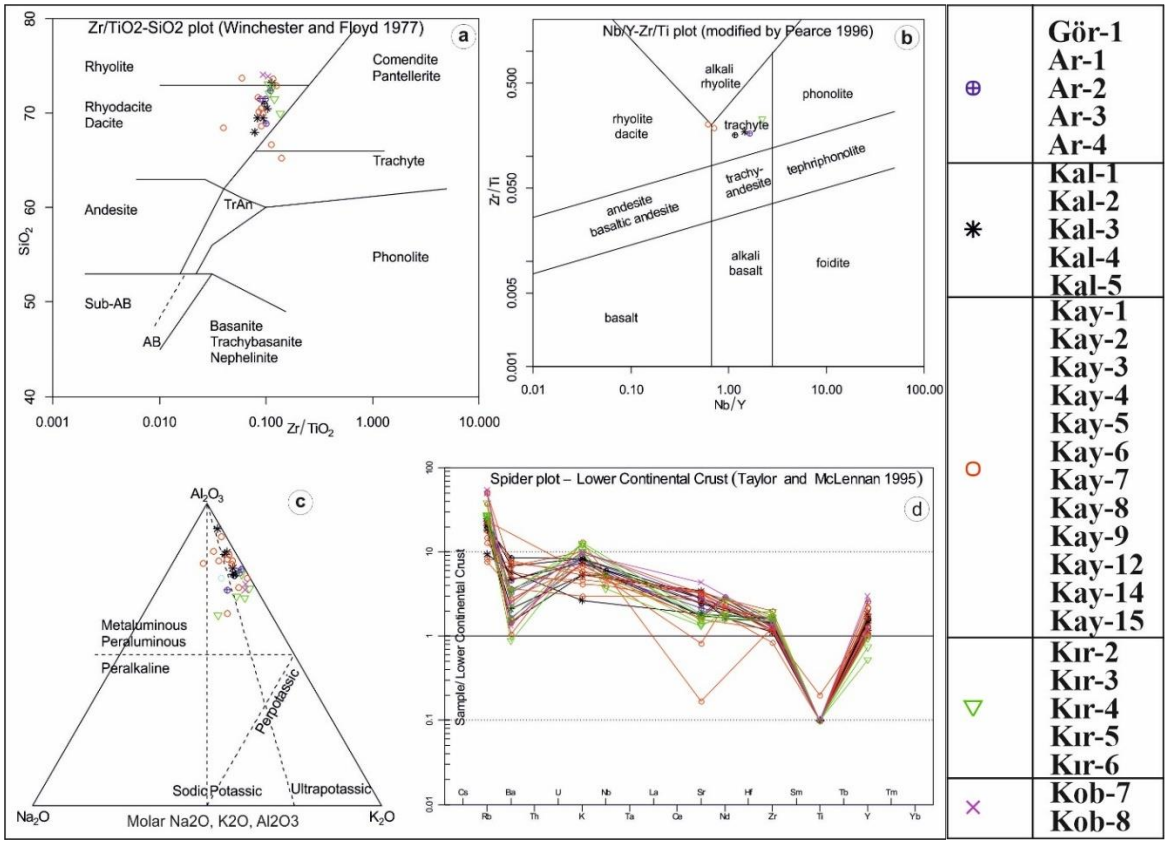

Figure 6. Relevant geological setting diagrams.

3.3. Evaluation of Gördes zeolites from an environmental perpective

Environmental issues have been an important subjects of humanity since the end of the 19th century and the first years of the 20th century [62–65]. Today, exploration of new raw materials is as important as the environmental impact during the actual exploitation, operation and processing of this raw material has become an important issue. Natural zeolite mines and their processing facilities do not present serious environmental problems with two exceptions [66]. These exceptions are fibrous zeolite

minerals and the presence of silica dusts formed during the exploitation and processing of zeolites. Erionite and mordenite minerals, as they are in the fibrous crystal system. Although fibrous erionite is aggreed to be Class 1 carcinogenic, there are still uncertainties regarding mordenite. Crystalline silicas are often found in zeolite deposits, which contain more than 1% material of respirable size. Therefore, these small-sized materials can interfere with the atmosphere and impair air quality. Despite all these negativities, zeolite minerals are generally inert and nonfibrous. Erionite, as stated, is a fibrous and acicular mineral. In the Cappadocia region (Aksaray, Niğde, Nevşehir cities) of Turkey, there are studies on carcinogenic effect of erionite. Although mordenite is also fibrous, no recorded cases of cancer related to mordenite have been encountered.

As the zeolite minerals in the study area, clinoptilolite is predominant, and the secondary abundant zeolite mineral is heulandite. Mordenite was found in only one sample at its location. Therefore, the field does not pose an environmental risk due to fibrous zeolite minerals. However, during the zeolite operation and processing activities, as in other open pit operations, attention should be paid to the relevant legislation, and the silica dust that will reduce the air quality should be prevented from entering the air.

Another environmental disadvantage of processes such as zeolitization and hydrothermal alteration is the change in the physicochemical conditions in the environment depending on the exposure of the rocks and the negative effects of some elements enriching in the environment while some of them move away from the environment under these conditions. Recently, there has been an increase in studies on these issues.

For this purpose, the element enrichment of the regions where zeolitisations were encountered in the field compared to the average upper crust [67] were examined (Fig. 7). When evaluated for Field V, it was seen that element V did not exceed the upper crust values at any sampling point. The Cr element was detected at only 5 sampling points, and in four of these locations, Cr values exceeded the upper crust values (92 ppm). This overrun occurred at a remarkable level, especially at Kay-2 and Kay-12 sampling points. It is thought that the fact that the volcanics in the field are more basic in character and that the Kay-12 sample point is located close to the IASZ ultrabasic rocks are effective for these overruns. No remarkable enrichment has been encountered in the field in terms of Zn element. It has been determined that the upper crust values are exceeded at most points in the field by the Rb, Sr and Y elements. When the field was evaluated in terms of the Ba element, it was determined that the Ba element exceeded the upper crust values in almost half of the sample points. It was observed that the Pb and Th elements were significantly higher at almost all of the sample points. U was found at only 4 sampling points and it was observed that U was remarkably higher than the upper crust values at all of these points. It is thought that the most important reason for the high values of these three elements compared to the upper crust values is related to the radioactive raw material potential of the region and the enrichment with these elements indicates the radiogenic origin. The geoaccumulation index (I_{geo}) and Pollution Index were calculated (according to [68] for the elements that are significantly higher than the upper crust values (Table 4). This parameter is calculated as follow; $I_{geo}=\log_2 Cn/1.5xBn$ that Cn is the concentrations of element at sampling point, Bn is the background concentration the element in upper continental crust of data from [67], and The constant number of 1.5 is the recommended correction factor for regional fluctuations for the elements.

Another pollution parameter is the Pollution Index (PI), that is defined as the ratio of element concentration in the area to the background value of the continental crust [69]. PIs of the elements were also calculated for the study are.
According to I_{geo}, <0 mean no risk of contamination. Between 0 and 1 are defined as unpolluted-moderately polluted, and above 1 as moderately and higher polluted. As to PI, PI parameter is classified as low (PI<1), medium (1<PI≤3 and high pollution risk (PI>3) [70].

When evaluated in terms of Igeo parameters, it has been observed that there is a moderately and higher polluted risk for Cr, Rb, Sr, Th at some sampling points of the field. For Pb and U, it has been determined that there is a medium-high pollution risk at all sample points with data. When the field is evaluated in terms of PI index, it is seen that the data obtained overlap with the Igeo data. The obtained findings suggest a more detailed investigation of heavy metal / radiogenic element contamination caused by alteration and / or zeolitisation in the field.

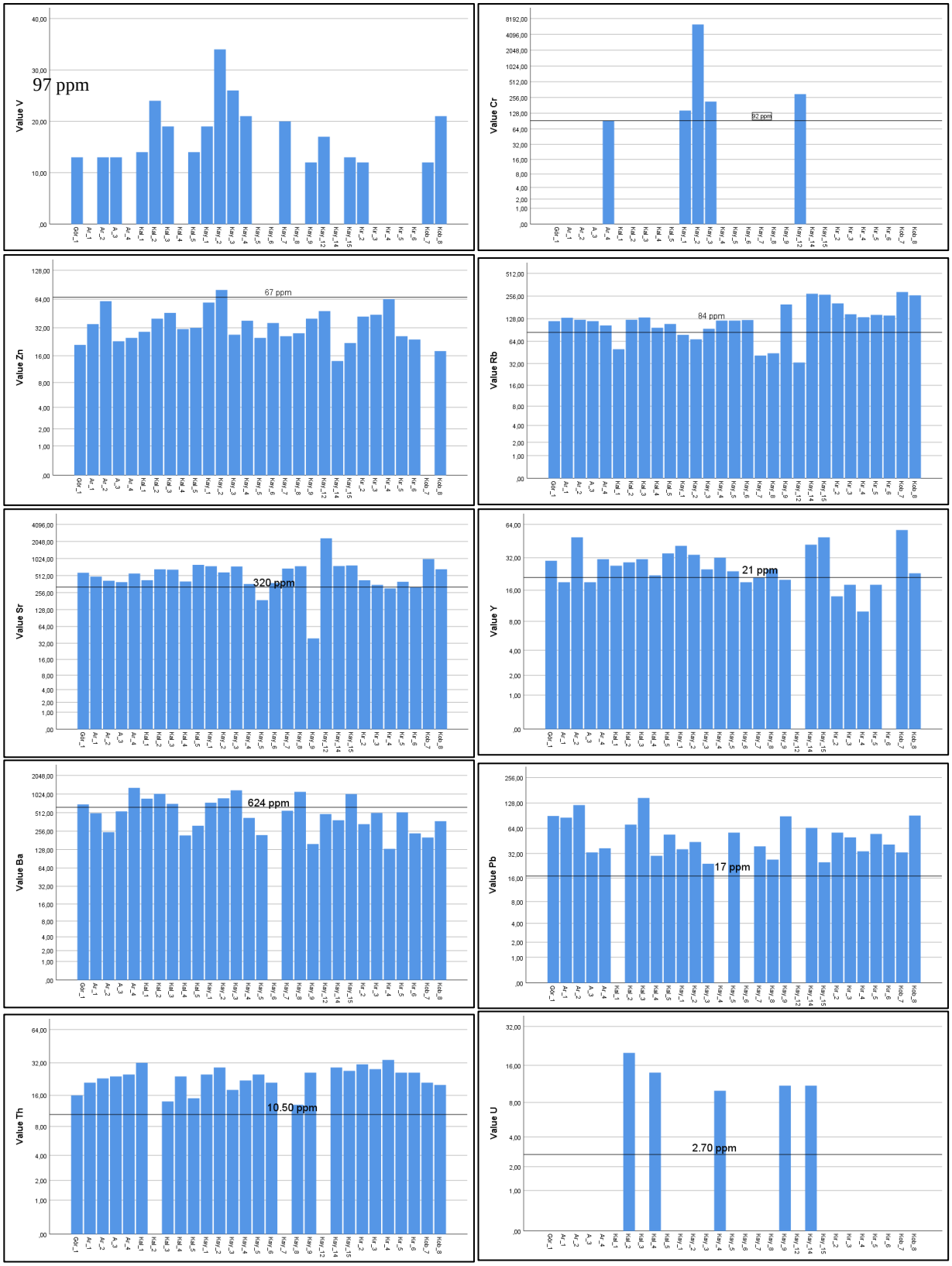

Figure 7. Bar diagrams with upper crust values [67] of the concentrations of elements according to the sampling points

Table 3. Igeo and PI values of the elements

	Igeo								PI							
	Cr_Igeo	Rb_Igeo	Sr_Igeo	Y_Igeo	Ba_Igeo	Pb_Igeo	Th_Igeo	U_Igeo	Cr__PI	Rb__PI	Sr__PI	Y__PI	Ba__PI	Pb__PI	Th__PI	U__PI
Gör_1		-0.08	0.26	-0.07	-0.43	1.82	0.02			1.42	1.80	1.43	1.11	5.29	1.52	
Ar_1		0.07	0.03	-0.73	-0.90	1.75	0.42			1.57	1.53	0.90	0.80	5.06	2.00	
Ar_2		-0.02	-0.21	0.64	-1.93	2.25	0.55			1.48	1.30	2.33	0.39	7.12	2.19	
A_3		-0.08	-0.29	-0.73	-0.80	0.37	0.61			1.42	1.23	0.90	0.86	1.94	2.29	
Ar_4	-0.60	-0.28	0.21	-0.02	0.46	0.54	0.67		0.99	1.24	1.74	1.48	2.07	2.18	2.38	
Kal_1		-1.33	-0.18	-0.22	-0.12		1.02			0.60	1.33	1.29	1.38		3.05	
Kal_2		-0.02	0.46	-0.12	0.14	1.48		2.30		1.48	2.06	1.38	1.65	4.18		7.41
Kal_3		0.08	0.44	-0.02	-0.40	2.53	-0.17			1.58	2.04	1.48	1.14	8.65	1.33	
Kal_4		-0.38	-0.26	-0.52	-2.10	0.23	0.61	1.79		1.15	1.26	1.05	0.35	1.76	2.29	5.19
Kal_5		-0.21	0.72	0.15	-1.58	1.08	-0.07			1.30	2.48	1.67	0.50	3.18	1.43	
Kay_1	0.06	-0.69	0.64	0.38	-0.34	0.50	0.67		1.57	0.93	2.34	1.95	1.19	2.12	2.38	
Kay_2	5.52	-0.89	0.28	0.11	-0.10	0.79	0.88		68.72	0.81	1.82	1.62	1.40	2.59	2.76	
Kay_3	0.63	-0.42	0.63	-0.33	0.33	-0.09	0.19		2.33	1.12	2.32	1.19	1.88	1.41	1.71	
Kay_4		-0.06	-0.40	0.02	-1.16		0.48	1.30		1.44	1.14	1.52	0.67		2.10	3.70
Kay_5		-0.06	-1.35	-0.39	-2.08	1.16	0.67			1.44	0.59	1.14	0.35	3.35	2.38	
Kay_6		-0.03	-0.34	-0.73			0.42			1.46	1.18	0.90			2.00	
Kay_7		-1.62	0.51	-0.58	-0.77	0.61				0.49	2.13	1.00	0.88	2.29		
Kay_8		-1.52	0.64	-0.33	0.25	0.08	-0.28			0.52	2.34	1.19	1.78	1.59	1.24	
Kay_9		0.65	-3.62	-0.66	-2.57	1.80	0.72	1.44		2.36	0.12	0.95	0.25	5.24	2.48	4.07
Kay_12	1.11	-1.93	2.28		-0.95				3.23	0.39	7.30		0.78			
Kay_14		1.13	0.65	0.42	-1.28	1.35	0.88	1.44		3.27	2.36	2.00	0.62	3.82	2.76	4.07
Kay_15		1.08	0.69	0.64	0.13	-0.03	0.78			3.18	2.42	2.33	1.64	1.47	2.57	
Kır_2		0.70	-0.18	-1.17	-1.49	1.16	0.98			2.44	1.32	0.67	0.53	3.35	2.95	
Kır_3		0.22	-0.45	-0.81	-0.89	0.97	0.83			1.75	1.10	0.86	0.81	2.94	2.67	
Kır_4		0.09	-0.66	-1.66	-2.83	0.42	1.11			1.60	0.95	0.48	0.21	2.00	3.24	
Kır_5		0.19	-0.27	-0.81	-0.86	1.11	0.72			1.71	1.24	0.86	0.83	3.24	2.48	
Kır_6		0.16	-0.59		-1.99	0.69	0.72			1.68	1.00		0.38	2.41	2.48	
Kob_7		1.20	1.06	0.86	-2.21	0.37	0.42			3.45	3.13	2.71	0.32	1.94	2.00	
Kob_8		1.06	0.47	-0.45	-1.33	1.84	0.34			3.12	2.07	1.10	0.60	5.35	1.90	

Igeo		PI	
Igeo<0	no risk of contamination	PI<1	Low pollution risk
0<Igeo≤1	unpolluted-moderately polluted	1<PI≤3	Medium pollution risk
Igeo>1	moderately and higher polluted	PI>3	Hig pollution risk

4.Conclusion

In this study, the evaluation of the zeolites in the Gördes basin in terms of their geological, geochemical, mineralogical and environmental effects has been carried out. As a result of the mineralogical-petrographic studies and XRD analysis, it was determined that the zeolite minerals in the field are mainly clinoptilolite and to a lesser extent heulandite. In a very limited sample, the presence of zeolite mineral mordenite (?)was found. Clinoptilolite and heulandite minerals were found together in some sampling locations. It was determined that the SEM-EDX analyzes confirmed the XRD results and that the zeolite minerals had a tabular crystal structure, not a fibrous crystal structure. It has been understood that the LOI values of the rocks are considerably higher than 5%, so the rocks absorb water into their crystal structures due to intense hydrothermal alteration and zeolitization processes. On the other hand, the pH data (6,97 to 9,91) show that the zeolite locations in the field are close to neutral to slightly basic. Major element distributions illustrating on Harker variation diagrams show that K_2O increase with increasing iO_2 and display positive trends compatible with the alteration process and zeolitization. On the Zr/TiO_2 versus SiO_2 diagram of [19] and the Nb/Y versus Zr/Ti diagram of [20], the zeolite bearing volcanic rocks are mainly rhyolitic, rhyodacitic and less commonly trachytic composition. As to molar Na_2O-K_2O-Al_2O_3 triangular diagram, all samples display metaluminous/peraluminous and potassic trend compatible with hydrothermal alteration/zeolitization process too.

When the zeolitisations in the study area are evaluated in terms of their environmental impact, According to both Igeo and PI parameters of the site, it was observed that the Cr, Rb, Sr and Th elements had a medium-high pollution risk, and the site had a significant pollution risk by Pb and U elements. It was concluded that the contamination in terms of Th, U and Pb in the field was caused by radiogenic and / or alteration, and the pollution risk observed by other elements was caused by zeolitisation / hydrothermal alteration. However, it is considered that more detailed studies should be carried out in this context in the field.

Acknowledgement

This study is supported by General Directorate of Mineral Research and Exploration (MTA, Ankara-Turkey). Authors thank to all MTA's officials. Authors also thank the editor and the anonymous reviewers for their improvement of the manuscript.

References

[1] Yücel H. Zeolitler ve Uygulama Alanları. 1987:391–402.

[2] Velde B, Pierre B. Soils, Plants and Clay Minerals Mineral and Biologic Interactions. Springer Berlin Heidelberg; 2010.

[3] Kayabalı K. Engineering aspects of a novel landfill material: Bentonite amended natural. Engineering Geology 1997; 46.

[4] Iijima A. Geology of natural zeolites and zeolitic rocks. Proceedings of the Filth International Conference on Zeo- IRes. Naples, Italy: 1980:103–108.

[5] Bish F, Guthrie G. Clays and zeolites. In: G.D. Guthrie and B.T. Mossmann (ed.), Health Effects of Mineral Dusts. Rev. Mineral. 1994:28:168-184.

[6] Esenli F, Özperek I. Zeolitic diagenesis of the Neogene basin in the vicinity of Gördes and mineralogy of heulandite- clinoptinolite. Bull Geol Congress Turkey 1993; 8:1–18.

[7] Vural A. Avliyana (Torul-Gümüşhane) Antimonit Cevherleşmesinin Jeolojisi-Mineralojisi ve Kökeninin Araştırılması. Gümüşhane: 2016.

[8] Albayrak M. Manisa (Gördes) bölgesi zeolitlerinin mineralojik, kimyasal ve teknolojik incelenmesi. Kibited 2010; 1:273–285.

[9] Vural A, Albayrak M. Gördes ve Çevresi Zeolitlerinin Mineralojisi. 58. Türkiye Jeoloji Kurultayı (58th Geological Congress of Turkey) (11-17 Nisan 2005). Ankara, Türkiye: 2005:140–141.

[10] Esenli F. Geological, mineralogical, and geochemical investigation of Neogene series and zeolitization in the vicinity of Gördes. Istanbul, Turkey: 1992.

[11] Türkbileği H. İzmir (Cumaovası-Urla-Çeşme-Karaburun) ve Manisa (Gördes Akhisar) zeolit yatakları maden jeolojisi raporu. Ankara: 1988.

[12] Albayrak M. Batı Anadolu, Trakya, Kapadokya Yöresi Zeolitleri Mineralojik Veri Kitabı. Ankara: 2008.

[13] Vural A, Aydal D. Determination of Lithological Differences and Hydrothermal Alteration Areas by Remote Sensing Studies: Kısacık (Ayvacık-Çanakkale, Biga Peninsula, Turkey). Journal of Engineering Research and Applied Science 2020.

[14] Aydal D, Vural A, Taşdelen-Uslu İ, Aydal, Emine G. Crosta Tecninique Aplication on Bayramic (Alakeçi-Kisacik) Mineralized Area By Using Landsat 7 TM Data. 30th Anniversary Fikret Kurtman Geology Symposium, Selçuk Univ. Geology Eng. Dep. Absracts Book, (in Turkish with English abstract). 2006:195.

[15] Aydal D, Vural A, Polat O. Definition Of The Base Metal And Gold Bearing Hydrotermally Altered Areas In Volcanic Rocks Using By Landsat 7 TM Imagery: Case Study From Bayramiç (Çanakkale). Abstracts of 57th Geology Congress, Turkey,. Turkey: 2004:89–90.

[16] Aydal D, Vural A, Taşdelen-Uslu İ, Aydal, Emine G. Investigation of Kuşçayırı-Kartaldağı (Bayramiç-Çanakkale) mineral enhancement region by Crosta technique with LANDSAT 7 ETM+ bands. Technical University of İstanbul, First Remote Sensing Workshop and panel book, 11p in Turkish with English abstract. 2006.

[17] Aydal D, Vural A, Taşdelen-Uslu İ, Aydal, Emine G. Crosta Technique Application On Bayramic (Alakeçi-Kısacık) Mineralized Area By Using Landsat 7 Etm+ Data. J FacEngArch Selcuk Univ 2007; 22:29–40.

[18] Corumluoglu O, Vural A, Asri I. Determination of Kula basalts (geosite) in Turkey using remote sensing techniques. Arabian Journal of Geosciences 2015; 8:10105–10117.

[19] Vural A, Corumluoglu O, Asri İ. Exploring Gördes Zeolite Sites by Feature Oriented Principle Component Analysis of LANDSAT Images. Caspian Journal of Environmental Sciences 2016; 14:285–298.

[20] Vural A, Corumluoglu O, Asri I. Zeolitleşmelerin Uzaktan Algılama Metotlarıyla Tespit Edilmesi: Gördes (Manisa) Örneği. 14. Türkiye Harita Bilimsel ve Teknik Kurultayı. 2013.

[21] Okay Aİ, Harris NBW, Kelley SP. Exhumation of blueschists along a Tethyan suture in northwest Turkey. Tectonophysics 1998; 285:275–299.

[22] Candan O, Çetinkaplan M, Oberhänsli R, Rimmelé G, Akal C. Alpine high-P/low-T metamorphism of the Afyon Zone and implications for the metamorphic evolution of Western Anatolia, Turkey. Lithos 2005; 84:102–124.

[23] Şengör AMC, Satır M, Akkök R. Timing of tectonic events in the Menderes Massif, western Turkey: implications for tectonic evolution and evidence for Pan- African basement in Turkey. Tectonics 1984; 3:693–707.

[24] Stampli GM, Borel GD. A plate tectonic model for the Paleozoic and Mesozoic constrained by dynamic plate boundaries and restored synthetic oceanic isochrones. Earth and Planetary Science Letters 2002; 196:17–33.

[25] Candan O, Koralay OE, Topuz G, Oberhänsli R, Fritz H, Collins AS, Chen F. Late Neoproterozoic gabbro emplacement followed by early Cambrian eclogite-facies metamorphism in the Menderes Massif (W. Turkey): Implications on the final assembly of Gondwana. Gondwana Research 2016; 34:158–173.

[26] Bingöl E. Geotechnical Evolution of Western Anatolia. Bulletin of the Mineral Research and Exploration 1976; 86:14–34.

[27] Candan O, Oberhänsli R, Dora OÖ, Çetinkaplan M, Koralay E, Rimmelé G, Chen F, Akal C. Polymetamorphic Evolution of the Pan-African Basement and Palaeozoic–Early Tertiary Cover Series of the Menderes Massif. Bulletin Of The Mineral Research and Exploration 2011; 142:121–163.

[28] Candan O, Dora OÖ, Oberhänsli R, Koralay E, Çetinkaplan M, Akal C, Satir M, Chen F. Menderes Masifinin Pan-Afrikan Temelinin Stratigrafisi Ve Gondvana'nın Geç Neoproterozoyik / Kambriyen Evrimi ile ilişkisi. Bulletin of Mineral Research and Exploration 2011; 142:25–68.

[29] Brinkmann R. Geotektonische Gliederung von Westanatolien. Neues Jahrbuch Fur Geologie Und Palaontologie - Abhandlungen 1966:603–618.

[30] Schuiling RD. Türkiye'nin Güneybatısındaki Menderes Masifi Migmatitik Kompleksinin Petrolojisi, Yapısı ve Yaşı Hakkında. Bulletin of Mineral Research and Exploration 1962; 58:71–84.

[31] Konak N, Akdeniz N, Öztürk EM. Geology of South Menderes Masifi Guide Book for Field. Excursion along Western Anatolia, Turkey. Ankara, Türkiye: 1987.

[32] Oberhänsli R, Candan O, Dora OÖ, Dürr SH. Eclogites within the Menderes Massif/western Turkey. Lithos 1997; 41:135–150.

[33] Dora O, Candan O, Kaya O, Koralay E, Dürr S. Revision of "Leptite-gneisses" in the Menderes Massif: A supracrustal metasedimentary origin. International Journal of Earth Sciences 2001; 89:836–851.

[34] Çağlayan MA, Öztürk EM, Sav H, Akat U. Menderes Masifi'nin Güneyine ait Bulgular ve Yapısal Yorum. TMMOB JMO Yayını Sayı 10; 1980.

[35] Hetzel R, Reischmann T. Intrusion age of Pan-African augen gneiss in the southern Menderes Massif and the age of cooling after Alpine ductile exten-sional metamorphism. Geological Magazine 1996; 133:505–572.

[36] Akkök R. Structural and metamorphic evolution of the northern part of the Menderes Massif: New data from the Derbent area and their implication for the tectonics of the massif. Journal of Geology 1983; 91:342–350.

[37] Dürr S. Über Alter und geotektonische Stellung des Menderes-Kristallins/SW-Anatolien und seine Äquivalente in der mittleren Aegaeis. University of Marburg, Lahn, 1975.

[38] Özer S, Sözbilir H, Özkar I, Toker V, Sari B. Stratigraphy of the Upper Cretaceous–

Palaeogene sequences in the southern and eastern Menderes Massif (western Turkey). International Journal of Earht Sciences 2001; 89:852–866.

[39] Oberhänsli R, Candan O, Wilke F. Menderes Masifinin orta kesimindeki Pan-Afrikan eklojitlerine ait jeokronolojik veriler. Turkish Journal of Earth Sciences 2010; 19:431–447.

[40] Dannat C. Geochemie, geochronologie und Nd-Sm Isotopie der granitoiden Kerngneiss des Menderes Massivs, SW-Turkey. , Johannes Gutenberg Universitat Mainz, 1997.

[41] Koralay OE. Geology, geochemistry and geochronology of granitic gneisses and leucocratic orthogneisses at the eastern part of Ödemiþ-Kiraz submassif, Menderes Massif: Pan-African and Triassic magmatic activities. Graduate School of Natural Science, Dokuz Eylül University, İzmir, 2001.

[42] Seyitoğlu G, Scott BC. Age of Alaşehir graben (west Turkey) and its tectonic implications. Geological Journal 1996; 31:1–11.

[43] Hetzel R, Ring U, Akal C, Troesch M. Miocene NNE-directed extensional unroofing in the Menderes massif, southwestern Turkey. Journal of Geological Society London 1995; 152:639–654.

[44] Candan O, Koralay OE, Akal C, Kaya O, Oberhänsli R, Dora OÖ, Konak N, Chen F. Supra-Pan-African unconformity between core and cover series of the Menderes Massif/Turkey and its geological implications. Precambrian Research 2011; 184:1–23.

[45] Ersoy YE, Helvaci C, Palmer MR. Stratigraphic, structural and geochemical features of the NE-SW trending Neogene volcano-sedimentary basins in western Anatolia: Implications for associations of supra-detachment and transtensional strike-slip basin formation in extensional tectonic setti. Journal of Asian Earth Sciences 2011; 41:159–183.

[46] Purvis M. The Late Tertiary–Recent tectonic-sedimentary evolution of extensional sedimentary basins of the Northern Menderes Massif. 1998.

[47] Şengör A, Yılmaz Y. Tethyan evolution of Turkey: a plate tectonic approach. Tectonophysics 1981; 75:181–241.

[48] Göktaş F. Gördes Neojen Havzasının Jeolojisi. Ankara: 1996.

[49] Seyitoğlu G. Late Cenozoic tectono-sedimentary development of the Selendi and Uşak-Güre basins: a contribution to the discussion on the development of east–west and north trending basins in western Turkey. Geological Magazine 1997; 134:163–175.

[50] Yılmaz Y, Genç ŞC, Gürer F, Bozcu M, Yılmaz K, Karacık Z, Altunkaynak Ş, Elmas A. When did the Western Anatolian grabens begin to develop? In: Bozkurt, E. Winchester, J.A., Piper J.A.D. (Eds.), Tectonics and Magmatism in Turkey and the Surrounding Area. Journal of Geological Society of London 2000; 173:131–162.

[61] Taylor SR, McLennan SM. The geochemical evolution of the continental crust. Reviews of Geophysics 1995; 33:241–265.

[62] Vural A, Ural MN, Çiftçi A. Kalkınma ve Çevre Konuları ile İlişkili Bazı Kavramların N-Gram Analizi ile Tarihsel Gelişiminin Değerlendirilmesi (Evaluation of Historical Development of Some Concepts Related to Development and Environmental Issues with N-Gram Analysis). International Black Sea Coastline Countries Symposium-5. Zonguldak, Türkiye: 2020:58–59.

[63] Vural A. Investigation of the radiation risk to the inhabitants in the region close to the hydrothermal alteration site, Gümüşhane/Turkey. Journal of Engineering Research and Applied Science 2019; 8:1168–1176.

[64] Vural A, Ural M, Çiftçi A. Evaluation of Historical Development of Some Concepts Related To Development And Environmental Issues with N-Gram Analysis. International Black Sea Coastline Countries Scientific Research Symposium- V. November 28-29, 2020 / Zonguldak, Turkey. 2020.

[65] Vural A, Ural MN, Çiftçi A. Analysis of Some Concepts Related to the Environment and Health with the N-Gram Method. Journal of International Health Sciences and Management 2020; (in press).

[66] Kogel JE, Trivedi NC, Barker JM, Krukowski ST. Industrial Minerals & Rocks Commodities, Markets and Uses. 2006.

[67] Rudnick R, Gao S. Composition of the Continental Crust. In: Holland H, Turekian K (eds.), Readings of Treatise on Geochemistry. 2nd ed. Londan, England: Elsevier; 2010.

[68] Muller G. Index of geoaccumulation in sediments of the Rhine River. Geological Journal 1969; 2:108–118.

[69] Chen CW, Kao CM, Chen CF, Dong C Di. Distribution and accumulation of heavy metals in the sediments of Kaohsiung Harbor, Taiwan. Chemosphere 2007; 66:1431–1440.
[70] Vural A. Contamination assessment of heavy metals associated with an alteration area: Demirören Gumushane, NE Turkey. Journal of the Geological Society of India 2015; 86:215–222.